HHS Public Access

Author manuscript

J Photochem Photobiol B. Author manuscript; available in PMC 2018 March 01.

Published in final edited form as:

J Photochem Photobiol B. 2017 March ; 168: 185–192. doi:10.1016/j.jphotobiol.2017.02.013.

Cationic dendritic starch as a vehicle for photodynamic therapy and siRNA co-delivery

Sarah A Engelberth[a], **Nadine Hempel**[b,*], and **Magnus Bergkvist**[a,*]

[a]Nanobioscience Constellation, Colleges of Nanoscale Science and Engineering, SUNY Polytechnic Institute, Albany NY 12203

[b]Department of Pharmacology, Penn State College of Medicine, Hershey, PA 17033

Abstract

Cationic enzymatically synthesized glycogen (cESG) is a naturally-derived, nano-scale carbohydrate dendrite that has shown promise as a cellular delivery vehicle owing to its flexibility in chemical modifications, biocompatibility and relative low cost. In the present work, cESG was modified and evaluated as a vehicle for tetraphenylporphinesulfonate (TPPS) in order to improve cellular delivery of this photosensitizer and investigate the feasibility of co-delivery with short interfering ribonucleic acid (siRNA). TPPS was electrostatically condensed with cESG, resulting in a sub-50 nm particle with a positive zeta potential of approximately 5 mV. When tested in normal ovarian surface epithelial and ovarian clear cell carcinoma cell culture models, encapsulation of TPPS in cESG significantly improved cell death in response to light treatment compared to free drug alone. Dosages as low as 0.16 μM TPPS resulted in cellular death upon illumination with a 4.8 J/cm^2 light dosage, decreasing viability by 96%. cESG-TPPS was then further evaluated as a co-delivery system with siRNA for potential combination therapy, by charge-based condensation of an siRNA directed at reducing expression of manganese superoxide dismutase (Sod2) as a proof of principle target. Simultaneous delivery of TPPS and siRNA was achieved, reducing Sod2 protein expression to 48%, while maintaining the photodynamic properties of TPPS under light exposure and maintaining low dark toxicity. This study demonstrates the versatility of cESG as a platform for dual delivery of small molecules and oligonucleotides, and the potential for further development of this system in combination therapy applications.

Graphical abstract

*Co-corresponding authors, to whom communication should be addressed. mbergkvist@sunypoly.edu, magnus.bergkvist@gmail.com and nhempel@psu.edu.

Supporting Information Available:

Conflict of Interest Disclosure: The authors declare no competing financial interest.

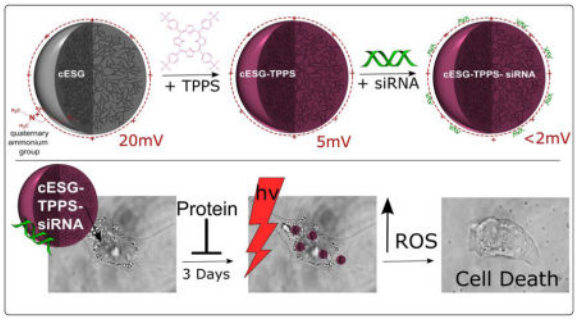

Keywords

Photodynamic therapy; sulfonated porphyrin; TPPS; co-delivery; siRNA; cationic enzymatically synthesized glycogen

1. Introduction

Photodynamic therapy (PDT) is a treatment modality that takes advantage of the activation of photosensitizers by light. Most commonly, light exposure results in oxygen radical production which elicits desired biological effects, most notably cytotoxicity. The first porphyrin photosensitizer for clinical use, Photofrin®, was approved for the treatment of papillary early stage bladder cancer in 1993 [1]. Since then, PDT applications have expanded to include a wide variety of cancers including prostate [2], head and neck [3–6], gastrointestinal [7], pancreatic [8], lung [9], and nonmelanoma skin cancer [10–13], as well as non-malignant conditions such as macular degeneration [14, 15] and psoriasis [16]. One obstacle in the clinical implementation of PDT (and other cancer therapies) is chemoresistance due to genetic aberrations and adaptations as a result of expression changes that confer a survival advantage to recurrent tumor populations [17]. Applying gene therapy in conjunction with PDT opens the possibility to tune the treatment to accommodate the genetic profile of the disease and target expression of proteins that may aid in chemoresistance. For example, in mouse xenograft models, knockdown of HIF1α (hypoxia-inducible factor 1-alpha) and VEGF-A (vascular endothelial growth factor A) have proven promising gene targets for improving photodynamic efficacy in head and neck cancer [18, 19] while downregulation of the protein DJ-1 has shown promise for ovarian cancer treatment [20]. Enhancement of PDT treatment by targeting disease-specific genes has also been demonstrated *in vitro* for urothelial [21] and breast cancer [22–24].

In previous work, our laboratory investigated the modification of enzymatically synthesized glycogen (ESG) as a cationic delivery vector for short interfering RNA (siRNA) to decrease targeted protein expression [25]. ESG is a naturally-derived, carbohydrate dendrite synthesized using *in vitro* enzymatic methods, resulting in a 20–40 nm diameter nanoparticle [26]. The dendrimeric glycan is highly branched and composed of α-glucose chains, bound by α1→4 glycosidic bonds, with α1→6 branching. Quaternary ammonium groups were introduced into cationic ESG (cESG, Figure 1) *via* epoxy chemistry to give a positively charged nanoparticle product with a zeta potential of about +20 mV. Electrostatically condensed cESG-siRNA successfully decreased expression of its target protein,

mitochondrial superoxide dismutase (Sod2), in an *in vitro* ovarian clear cell carcinoma model [25]. We have demonstrated that Sod2 maintains mitochondrial function and is important for ovarian cancer metastasis. Knock-down of this enzyme in ovarian cancer increases both accumulation of the superoxide anion in the mitochondria, and prevents superoxide conversion to H_2O_2, which abrogates H_2O_2 mediated signaling and migration. [27].

The primary aim of this study was to investigate whether chemically modified ESG can be considered as a delivery platform to load therapeutic modalities beyond siRNA. To test one such application we evaluated loading of the photosensitizer tetraphenylporphinesulfonate (TPPS) into cESG for PDT. In addition, the feasibility of co-delivery with siRNA was tested. TPPS (Figure 2) is an anionic, hydrophilic porphyrin that was first explored as a photosensitizer for cancer treatment in the 1960s, showing good tumor localization and photodynamic efficiency [28, 29]. However, *in vivo* studies revealed that systemic administration of TPPS induced neurotoxic effects [30]. Similar functional damage was observed with injection of Photofrin® and Levulan®, but this damage was reversible once they cleared circulation. Increased circulation time of TPPS, attributed to albumin binding, led to irreversible damage and structural changes in the peripheral nervous system [31]. Given this unwanted toxicity, TPPS formulation has, so far, not moved from the bench to the clinic. Electrostatic condensation of anionic TPPS to cargo vehicles has been demonstrated as a feasible mechanism for delivery, as observed in the retention of photobehavior of TPPS in both cationic amphiphilic cyclodextrin [32] and coiled peptides [33]. Thus we hypothesized that charge-based condensation of cESG may be a feasible strategy to encapsulate TPPS and retain functionality. cESG-mediated TPPS delivery was investigated in an ovarian cancer cell line model and improved light-induced death response and reduced dark-toxicity, compared to unconjugated TPPS. The flexibility of cESG as a potential PDT delivery vector was further demonstrated when siRNA was successfully conjugated and co-delivered with TPPS to cells in culture.

2. Experimental Procedures

2.1 Materials

Enzymatically synthesized glycogen (ESG, Bioglycogen™ lot 100526) was purchased from Glico Nutrition Co. Ltd. 5, 10, 15, 20-tetrakis(4-sulfonatophenyl)-21H,23H-porphyrin (TPPS) was purchased from Frontier Scientific. McCoy's 5A media, RPMI media, and Trypsin EDTA 1x were obtained from ATCC. Hyclone fetal bovine serum was purchased from GE Healthcare. Dulbecco's phosphate buffer saline 1x was obtained from ThermoFisher Scientific. A 5′ fluorescein 6-FAM-labeled, previously validated [27] siRNA targeting Sod2 was purchased from Dharmacon (On-Target Plus 5′-CAACAGGCCUUAUUCCACU-3′). A scramble oligonucleotide sequence was used as a non-targeting control (Dharmacon, OnTarget Plus Control siRNA Nontargeting siRNA #1). Antibodies were obtained from Cell Signaling Technology (Boston, MA) or Abcam (Cambridge, MA). Synthesis experiments were conducted using 18.2 MΩ•cm, RNAse free water. All experiments were conducted with reagent grade chemicals purchased from Sigma Aldrich, unless otherwise specified.

2.2 Synthesis of cESG

cESG was synthesized as described previously[25]. Briefly, ESG was reacted for 24 hours at room temperature in 0.1 M sodium phosphate buffer pH 12.5, at a 1:10 molar ratio of Anhydrous Glucose Units:GTMA. The product was purified by dialysis against 1 mM sodium chloride with at least 3 volume exchanges, and lyophilized on a Labconco Freezone 2.5 Plus.

2.3 Condensation of cESG-TPPS

Lyophilized cESG was dissolved in 1 mM $NaPO_4$ buffer pH 7.5 at a particle concentration of 0.78 μM (8 mg/mL). Stock 10 mM TPPS, prepared in distilled water, was added to the solution at a range of concentrations (6.25, 12.5, 25, and 50 μM). Solutions were stirred overnight in glass vials at room temperature. Products were dialyzed in 10 kDa MWCO regenerated cellulose membrane (ThermoScientific) for 24 h against 4 L of distilled water to remove free TPPS. Samples were then lyophilized using a Labconco Freezone 2.5 Plus and resuspended to desired concentrations in 1 mM sodium phosphate buffer pH 5.7 for further analysis.

2.4 Absorbance and Fluorescence Studies

Spectroscopic studies were conducted in a 96-well half area plate on a SpectraMax Paradigm plate reader (Molecular Devices). For absorbance measurement, samples were diluted 1:50 in 20 mM sodium phosphate buffer pH 9. Absorbance at 417 nm was read and spectra were collected from 350–500 nm with a 1 nm step size. A TPPS standard curve (0 to 5 μM) in the same buffer was generated using the same instrumentation and used to calculate TPPS concentration in cESG samples. For fluorescence measurement, all compounds were diluted to a concentration of 3 μM TPPS. Fluorescence emission spectra (420 nm excitation) were collected from 450–650 nm with a 1 nm step size.

2.5 Gel Permeation Chromatography (GPC)

100 μL of cESG-TPPS was loaded onto a Sephadex G-25 crosslinked dextran desalting column with 2.5 mL void volume (GE Healthcare). 20 mM sodium phosphate buffer pH 9 was added up to a 2 mL volume. Eight 250 μL fractions were collected, followed by the additional collection of four 500 μL fractions. Free TPPS bound to the column and did not elute. Absorbance (at 417 nm) was used to calculate the concentration of particle-bound TPPS in each fraction using the same standard curve as described above. The concentration of bound TPPS (μM) in the original sample was calculated by equation 1. Binding efficiency was calculated using equation 2.

$$\frac{\sum (uM\ \ Concentration * Fraction\ \ Volume)}{Initial\ \ Sample\ \ Volume} = uM\ TPPS\ Bound \quad \text{(Equation 1)}$$

$$\frac{Concentration\ TPPS\ Bound}{Concentration\ TPPS\ Added} * 100\% = Binding\ Efficiency \quad \text{(Equation 2)}$$

2.6 Dynamic Light Scattering (DLS)

Zeta (ζ) potential and mean particle diameter were determined in 1 mM sodium phosphate buffer pH 7.5 using DLS (Malvern Zetasizer Nano, Worcestershire, UK). Mean particle diameter measurements were averaged over three measurements using 15 scans at 5 seconds each. The particle diameters reported were calculated by the percent volume algorithm of the Malvern Zetasizer collection software. Zeta potential measurements at 40 mV electrode potential were averaged over three measurements of 30 runs each.

2.7 Cell Culture

The ES-2 ovarian clear cell ovarian carcinoma cell line was purchased from ATCC. Nose007, normal ovarian surface epithelial cells, were kindly provided by Dr. Susan K. Murphy (Duke University). Cells were maintained in McCoy's 5A medium or RPMI medium, respectively, supplemented with 10% fetal bovine serum, penicillin (100 U/L) and streptomycin (0.1 mg/L), and cultured at 37 °C under 5% CO_2.

2.8 Testing the PDT Efficacy of cESG-TPPS Particles on Cell Viability

ES-2 and Nose007 cells were seeded into 96-well plates at a density of 4,000 cells per well. The following day, cells were treated in growth media using cESG-TPPS at a concentration of 0.72 μM bound TPPS (to 2.7 nM cESG) with 0.28 μM free TPPS remaining in solution, totaling 1 μM TPPS treatment in the well. A control 1 μM unbound ("free") TPPS treatment was also conducted. After 24 hour incubation the treatment solution was aspirated from the cells and replaced with fresh growth media. Cells were then illuminated with a 630 nm 8 mW/cm^2 LED lamp positioned 0.5 cm above the plate for 0 (dark control), 5, or 10 minutes. The following day, an MTT cell viability assay (ThermoFisher Scientific) was performed to determine cell viability. To evaluate the effect of bound TPPS dosage, a similar experiment was performed on ES-2 cells treated with cESG-TPPS at a constant 3.2 nM cESG concentration and variable bound TPPS concentrations (0.16, 0.32, and 0.72 μM bound TPPS) with a total TPPS concentration in solution of 1 μM. Generation of free radicals in the system was tested by quenching singlet oxygen according to the method used by Hirohara et al [34]. Briefly, After a 24 h incubation with 1 μM cESG-TPPS or free TPPS compounds, the treatments were removed and replaced with either 5 mM sodium azide (a singlet oxygen scavenger) or growth media and incubated for 2 h. Wells were illuminated for 10 minutes as described above and an MTT assay conducted.

2.9 Gel Shift Assay for Condensation of cESG-TPPS with siRNA

100 ng of siRNA (Sod2-specific targeting sequence with a fluorescein-label) was mixed with cESG-TPPS at either a 1:1, 4:1 or 8:1 molar ratio siRNA:cESG and diluted to a final volume of 14 μL using 1 mM sodium phosphate buffer (final siRNA concentration 0.5 μM). Formulations had either 24 or 42 TPPS per particle, with final cESG concentrations of 500, 125, and 60 nM respectively. Reactions were incubated for 40 min, vortexing every 5 min to facilitate mixing and siRNA incorporation. Then, 10 μL of reaction was mixed with 2 μL of 10x loading buffer and loaded into a 1% agarose gel containing ethidium bromide. The gel was run in 1% TAE buffer at 100 V for approximately 20 min, followed by ethidium

bromide staining for an additional 10–15 min. Gels were imaged on a FluorChem E imager (Protein Simple).

2.10 Evaluating cESG-TPPS-siRNA Particles for PDT

ES-2 cells were seeded into 96-well plates at a density of 4,000 cells per well. The following day, cells were treated with cESG-TPPS-siRNA condensed immediately before treatment (10 nM siRNA, 15.2 nM cESG, and variable TPPS concentration). Final bound TPPS concentrations for treatment were 1.1, 0.46, 0.32, and 0.17 μM. Treatments using cESG-TPPS without siRNA were performed simultaneously for comparison. Cells were incubated with 100 μL of treatment solution for 3 days at 37 °C. Then solutions were replaced with fresh growth media and illuminated with a 630 nm 8 mW/cm^2 LED lamp positioned 0.5 cm above the plate for 0 or 10 min. The following day, an MTT assay was conducted to determine cell viability.

2.11 Evaluation of Sod2 Protein Expression Following cESG-TPPS-siRNA-mediated Knockdown

ES-2 cells were seeded into 6-well plates at a density of 80,000 cells per well. The following day, cESG-TPPS-siRNA complexes were condensed immediately prior to treatment, at a 1:4 molar ratio as described above. Controls included cESG alone, cESG-TPPS, and cESG-TPPS-siRNA-scramble. Treatments were conducted in growth media for 3 days (10 nM siRNA, 15.2 nM cESG) followed by imaging and western blot analysis as described previously [25]. Uptake of the complex was assessed by fluorescence of the TPPS (420/507 ex/em, pH 9) using an AMG EVOS$_{fl}$ microscope with Texas Red LED light source filter cube, using a 20x objective. Bright field images were taken simultaneously and the percentage of fluorescent cells quantified using ImageJ.

2.12 Calculation and Statistical Analysis

All data presented are representative of at least three independent experiments and expressed as mean ± SEM, unless otherwise noted. Statistical data analyses were performed using OriginPro Software v8.5. One-way ANOVA with Tukey’s post-hoc test were performed as indicated.

3. Results

3.1 TPPS Incorporation into cESG

The charge-based encapsulation of TPPS with cESG was investigated using an overnight, room temperature reaction. As TPPS is highly water soluble, dialysis was attempted to remove unbound TPPS and UV-Vis absorbance used to determine the concentration of remaining TPPS. At neutral pH, stacking of the TPPS in solution occurred. Some of these aggregates were larger than the pores of dialysis tubing, resulting in TPPS not associated with cESG to remain in the sample solution. As such, gel permeation chromatography (GPC) was used as an alternative method to determine the concentration of TPPS bound to cESG. In this method, anionic free TPPS was trapped in the dextran column matrix and did not elute. The cESG particles with bound TPPS eluted in the void volume and were detected in early fractions using UV-Vis absorbance (Figure 3).

The concentration of TPPS bound was calculated using equation 1, showing a linear relationship between the concentration of TPPS added and the amount of TPPS associated with cESG (Supplemental Figure 1). At lower TPPS concentrations, 6 μM and 12 μM, all molecules bound to the cESG (100% binding efficiency, equation 2). As more TPPS was added, the binding efficiency decreased to 76% and 66% at 25 μM and 50 μM, respectively. DLS analysis of the cESG-TPPS complex indicated all samples were 35–45 nm in diameter, indicating individual particles had a similar size to cESG alone (Table 1). The zeta potential of cESG decreased from +20 mV down to +4–5 mV upon TPPS incorporation at all conditions tested (Table 1).

3.2 Spectroscopic Characterization of cESG-TPPS

In order to test if TPPS retained light adsorption and emission behavior once bound to cESG, absorbance and fluorescence spectra were collected. The absorbance spectrum of free TPPS (Figure 4A) had a Soret band at 413 nm with a small shoulder around 405 nm. The reported Soret band for monomeric TPPS species is located at 412 nm [35], but spectra often show a blue-shifted shoulder (406 nm) attributed to TPPS species aggregated in face-to-face dimer stacks [36]. In cESG-TPPS complexes, the Soret band was red shifted to 420 nm, with a decrease in absorbance intensity. cESG-TPPS also exhibited a corresponding redshift in the Q-bands located between 500–700 nm (Supplemental Figure 2), as discussed below. The fluorescence emission profile of cESG-TPPS also exhibited minor changes. The fluorescence maxima of TPPS alone had a right shoulder which was red-shifted to a distinct secondary peak at 568 nm in all cESG-TPPS formulations (Figure 4B), consistent with a change in TPPS conformation. There was an increase in the fluorescence intensity of cESG-TPPS complexes over free TPPS (Supplemental Figure 3), with the highest signal in formulations with the most TPPS per cESG.

3.3 Efficacy of cESG-TPPS for PDT

The efficacy of cESG-TPPS for PDT was tested in ES-2 ovarian cancer and Nose007 normal ovarian surface epithelial cells. Following an overnight incubation with treatment in growth media, cells were illuminated for 5 or 10 minutes (2.4 and 4.8 J/cm^2 light dosage respectively) and cell death response monitored using an MTT cell viability assay (Figure 5). Following light treatment there was statistically significant death ($p<0.001$) in both ES-2 and Nose007 cells at a 0.72 μM TPPS dosage of cESG-TPPS (encapsulated in 2.7 nM cESG). Due to incomplete purification during dialysis, there was additional 0.28 μM free TPPS remaining in solution. Thus the control TPPS treatment (free in solution) was conducted at a total 1 μM TPPS concentration, resulting in no significant cell death at this dosage. As such, cell death in cESG-TPPS treatment was attributed to the cESG-bound photosensitizer. No statistically significant difference ($p>0.05$) was observed between the different cell types, however there was an increase in dark toxicity in cESG-TPPS treatment of Nose007 cells. ES-2 cells were chosen for further analyses and the effect of decreasing TPPS dosage at constant cESG concentration was evaluated at a constant 3.2 nM cESG. Efficient PDT light response was observed at doses as low as 0.16 μM bound TPPS (Figure 6). Importantly, cESG-bound TPPS (green bars) significantly improved cytotoxicity over unencapsulated TPPS (blue bars). A slight increase in cell viability was observed with 0.72 μM cESG-TPPS, compared to the lower concentrations. However, the cell viability of the

corresponding controls for this set was also slightly higher. Despite a slight shift in viability of this group, it is clear that upon illumination encapsulated TPPS (green bars) caused significant ($p<0.01$) cell death compared to free TPPS (blue bars) at all dosages tested. Moreover, unencapsulated TPPS did not result in significant decreases in cell viability following illumination.

3.3 cESG-TPPS for siRNA co-delivery

Previous work in our laboratory has demonstrated cESG can successfully mediate siRNA delivery for expression knockdown of Sod2 [25]. Considering that cESG-TPPS formulations retained a positive zeta potential of approximately 5 mV (Table 1), charge-based condensation and co-delivery of siRNA were further investigated. Following a room temperature, 40 minute condensation of cESG-TPPS with siRNA, a gel shift assay revealed that siRNA was completely bound at multiple particle formulations (Supplemental Figure 4). Size and zeta potential analysis of the particle complexes indicate that there was no major aggregation induced by siRNA condensation, with zeta potentials shifting toward neutral (Table 2).

Once the ability of cESG-TPPS to bind siRNA was confirmed, experiments were carried out to determine the cellular uptake of this co-delivery system. cESG-TPPS-siRNA-Sod2 treatment was investigated in ES-2 cells using 42 TPPS per cESG particle. siRNA condensation was conducted immediately before treatment and cellular uptake in growth media assessed by the red fluorescent signal of TPPS. After a three day incubation, 90% of the cell population internalized cESG-TPPS and cESG-TPPS-siRNA formulations (Supplemental Figure 5). A three day incubation was conducted to ensure efficient knock down and degradation of existing endogenous Sod2 protein. Loss of Sod2 expression was assessed using western blotting. cESG-TPPS-siRNA-Sod2 successfully mediated Sod2 knockdown, with Sod2 expression decreasing to 48% of control levels (untreated control), in line with that reported for cESG-siRNA-Sod2 from our previous study (35% knock-down) [25] (Figure 7).

PDT efficiency of cESG-TPPS-siRNA was investigated to determine if there was a synergistic effect between Sod2 knockdown and TPPS treatment. Again, siRNA condensation was performed immediately prior to the treatment of the cells in growth media. All treatments were conducted for three days at constant cESG (17 nM) and siRNA (10 nM) levels, with varying TPPS concentrations. Following this incubation, cells were treated with 630 nm light for 10 minutes (4.8 J/cm^2) in fresh growth media. The next day, viability was assessed using an MTT assay. Both cESG-TPPS and cESG-TPPS-siRNA exhibited minimal dark toxicity (Figure 8). Upon illumination, cESG-TPPS and cESG-TPPS-siRNA were both effective at inducing cellular death, with higher responses at increasing TPPS dose. Cells with siRNA-mediated Sod2 knockdown showed no statistically significant difference in cell viability compared to cESG-TPPS treatment alone. However siRNA and TPPS were successfully co-delivered, and a trend, although not statistically significant, was observed in which decreased Sod2 protein expression slightly improved PDT sensitivity. It is of note that several experimental conditions were altered for use of cESG-TPPS for siRNA delivery when compared to cESG-TPPS for photodynamic therapy alone (Figure 6). In order to

achieve protein knockdown, the cells were incubated with the constructs for a longer period (72 hours rather than 24) and were treated with a higher concentration of cESG (15.2 nM rather than 3.2 nM) than in the previous experiment. This accounts for variation in cytotoxicity between siRNA conjugated (Figure 8) and unconjugated cESG (Figure 6).

4. Discussion

In this study, we demonstrated the ability of a cationic dendritic starch nanoparticle, cESG, to bind and deliver a small molecule therapeutic (TPPS photosensitizer). We also demonstrated the ability of cESG to co-deliver siRNA for potential combination therapy. Charge-based binding of TPPS was conducted by an overnight room temperature reaction, with resultant complexes retaining a positive zeta potential. Minor changes in spectroscopic absorbance and fluorescence characteristics of TPPS were observed upon cESG binding. A redshift (bathochromic shift) in the Soret band was observed, similar to that observed for TPPS J-aggregates (edge-by-edge or side-to-side stacks) formed at lower pH [36]. It is possible that the shift seen in cESG-TPPS is due to a similar mechanism, where the orientation of the exterior aromatic rings were rotated upon binding, leading to delocalization of π-electrons in the porphyrin core [37]. The increase in the fluorescence intensity of cESG-TPPS complexes over free TPPS indicated that binding did not lead to self-quenching. Rather, the binding may have prevented the formation of aggregates observed with free TPPS in solution.

The application of cESG-TPPS for PDT was explored in two different cell types. There was no statistically significant difference ($p>0.05$) between treatment in the normal ovarian epithelium (Nose007) and ovarian clear cell carcinoma (ES-2) cells. Treatment with 0.72 μM TPPS encapsulated in cESG resulted in less than 10 percent cell viability following illumination. When tested at constant cESG dosage and decreasing TPPS concentration, cESG-TPPS treatment effectively mediated cellular death at dosages as low as 0.16 μM. Free TPPS did not result in any cell death at these concentrations. A likely mechanism for the enhanced efficacy of TPPS conjugated to cESG may be the increased cellular uptake of the slightly positive-charged cESG-TPPS complex [38], compared to that of free TPPS.

Finally, condensation of cESG-TPPS with siRNA was established through sequential charge-based condensations. A 1:4 molar ratio of particle to siRNA was chosen for cell experiments based upon previous studies with cESG-siRNA [25]. Internalization of the cESG-TPPS-siRNA-Sod2 complex was seen in 90% of the ES-2 cell population. Sod2 knockdown was also demonstrated, decreasing Sod2 protein expression to 48%. This result demonstrates that cESG-TPPS can be used as a siRNA delivery vector for ES-2 cells while slightly less efficient at mediating protein expression than cESG-siRNA alone, which reduced protein expression to 35% [25].

In the ES-2 cell culture model, the co-delivery system was successful for both the delivery of siRNA, as evidenced by Sod2 knockdown, and TPPS, demonstrated by effective phototoxicity upon illumination. However, the incorporation and co-delivery of siRNA targeting Sod2 with cESG-TPPS did not further improve the light-induced toxicity on a significant level, suggesting that a loss of Sod2, and inability to scavenge superoxide, did not

lead to increased sensitivity to this PDT agent. The lack of clear synergistic effect between Sod2 knockdown and PDT treatment could be attributed to the mitochondrial localization of Sod2, as well as the type of ROS produced following TPPS photoactivation. It has previously been demonstrated that TPPS excitation primarily leads to the generation of singlet oxygen [39] rather than superoxide anion. Quenching of singlet oxygen in our system indicated that this is a major contributor to cellular death following illumination (Supplemental Figure 6). Nevertheless, this study verifies the flexibility of cESG for co-delivery of siRNA and small molecular therapeutics. In order to ablate resistant tumor populations during PDT, siRNA against different genetic targets, including cytosolic localized antioxidant enzymes and regulators of antioxidant expression, such as Nrf2 and DJ-1 [20], could be utilized with the system. This co-delivery platform could be further explored in conjunction with a wide range of other anionic therapeutics in order to improve patient outcomes.

Supplementary Material

Refer to Web version on PubMed Central for supplementary material.

Acknowledgments

The authors would like to acknowledge the SUNY Research Fund and NIH for funding (NIH/NCI grant R00CA143229 to NH).

Abbreviations

ESG
Enzymatically synthesized glycogen

cESG
cationic enzymatically synthesized glycogen

tetraphenylporphyrine sulfonate, TPPS
5,10,15,20-tetrakis(4-sulfonatophenyl)-21H,23H-porphyrin

GTMA
glycidyltrimethylammonium chloride

DLS
dynamic light scattering

siRNA
short interfering ribonucleic acid

References

1. Dougherty TJ. Photodynamic therapy. Photochemistry and photobiology. 1993; 58(6):895–900. [PubMed: 8310013]
2. Nathan TR, et al. Photodynamic therapy for prostate cancer recurrence after radiotherapy: a phase I study. The Journal of urology. 2002; 168(4):1427–1432. [PubMed: 12352410]

3. Prosst R, Wolfsen H, Gahlen J. Photodynamic therapy for esophageal diseases: a clinical update. Endoscopy. 2003; 35(12):1059–1068. [PubMed: 14648421]

4. Dilkes M, et al. Treatment of primary mucosal head and neck squamous cell carcinoma using photodynamic therapy: results after 25 treated cases. Journal of laryngology and otology. 2003; 117(9):713–717. [PubMed: 14561360]

5. Bellnier DA, et al. Population pharmacokinetics of the photodynamic therapy agent 2-[1-hexyloxyethyl]-2-devinyl pyropheophorbide-a in cancer patients. Cancer Research. 2003; 63(8): 1806–1813. [PubMed: 12702566]

6. Lorenz KJ, Maier H. Photodynamic therapy with meta-tetrahydroxyphenylchlorin (Foscan®) in the management of squamous cell carcinoma of the head and neck: experience with 35 patients. European Archives of Oto-Rhino-Laryngology. 2009; 266(12):1937–1944. [PubMed: 19290535]

7. Puolakkainen P, Schröder T. Photodynamic therapy of gastrointestinal tumors: a review. Digestive Diseases. 1992; 10(1):53–60. [PubMed: 1551247]

8. Moesta KT, et al. Evaluating the role of photodynamic therapy in the management of pancreatic cancer. Lasers in surgery and medicine. 1995; 16(1):84–92. [PubMed: 7536286]

9. Kato H. Photodynamic therapy for lung cancer—a review of 19 years' experience. Journal of Photochemistry and Photobiology B: Biology. 1998; 42(2):96–99.

10. Baas P, et al. Photodynamic therapy with meta-tetrahydroxyphenylchlorin for basal cell carcinoma: a phase I/II study. British Journal of Dermatology. 2001; 145(1):75–78. [PubMed: 11453910]

11. Zeitouni NC, Oseroff AR, Shieh S. Photodynamic therapy for nonmelanoma skin cancers: current review and update. Molecular immunology. 2003; 39(17):1133–1136. [PubMed: 12835091]

12. Schweitzer VG. Photofrin-Mediated Photodynamic Therapy for Treatment of Aggressive Head and Neck Nonmelanomatous Skin Tumors in Elderly Patients. The Laryngoscope. 2001; 111(6):1091–1098. [PubMed: 11404627]

13. Rhodes LE, et al. Photodynamic Therapy Using Topical Methyl Aminolevulinate vs Surgeryfor Nodular Basal Cell Carcinoma: Results of a Multicenter Randomized Prospective Trial. Archives of dermatology. 2004; 140(1):17–23. [PubMed: 14732655]

14. Rechtman E, et al. An update on photodynamic therapy in age-related macular degeneration. Expert opinion on pharmacotherapy. 2002; 3(7):931–938. [PubMed: 12083992]

15. Müller VA, et al. Treatment of Rubeosis iridis with Photodynamic Therapy with Verteporfin–A New Therapeutic and Prophylactic Option for Patients with the Risk of Neovascular Glaucoma? Ophthalmic research. 2003; 35(1):60–64. [PubMed: 12566865]

16. Szeimies R, Landthaler M, Karrer S. Non-oncologic indications for ALA-PDT. Journal of dermatological treatment. 2002; 13(sup1):s13–s18. [PubMed: 12060512]

17. Milla Sanabria L, et al. Direct and indirect photodynamic therapy effects on the cellular and molecular components of the tumor microenvironment. Biochim Biophys Acta. 2013; 1835(1):36–45. [PubMed: 23046998]

18. Chen WH, et al. Nanoparticle delivery of HIF1alpha siRNA combined with photodynamic therapy as a potential treatment strategy for head-and-neck cancer. Cancer Lett. 2015; 359(1):65–74. [PubMed: 25596376]

19. Lecaros RL, et al. Nanoparticle Delivered VEGF-A siRNA Enhances Photodynamic Therapy for Head and Neck Cancer Treatment. Mol Ther. 2016; 24(1):106–16. [PubMed: 26373346]

20. Schumann C, et al. ROS-induced nanotherapeutic approach for ovarian cancer treatment based on the combinatorial effect of photodynamic therapy and DJ-1 gene suppression. Nanomedicine. 2015; 11(8):1961–70. [PubMed: 26238076]

21. Miyake M, et al. siRNA-mediated Knockdown of the Heme Synthesis and Degradation Pathways: Modulation of Treatment Effect of 5-Aminolevulinic Acid-based Photodynamic Therapy in Urothelial Cancer Cell Lines. Photochemistry and Photobiology. 2009; 85:1020–1027. [PubMed: 19320847]

22. Dong D, et al. Therapeutic potential of targeted multifunctional nanocomplex co-delivery of siRNA and low-dose doxorubicin in breast cancer. Cancer Lett. 2015; 359(2):178–86. [PubMed: 25592040]

23. Jin G, et al. Multifunctional organic nanoparticles with aggregation-induced emission (AIE) characteristics for targeted photodynamic therapy and RNA interference therapy. Chem Commun (Camb). 2016; 52(13):2752–5. [PubMed: 26759835]
24. Cogno IS, et al. Optimization of photodynamic therapy response by survivin gene knockdown in human metastatic breast cancer T47D cells. J Photochem Photobiol B. 2011; 104(3):434–43. [PubMed: 21641815]
25. Engelberth SA, Hempel N, Bergkvist M. Chemically Modified Dendritic Starch: A Novel Nanomaterial for siRNA Delivery. Bioconjugate chemistry. 2015; 26(8):1766–1774. [PubMed: 26218732]
26. Kajiura H, et al. A novel enzymatic process for glycogen production. Biocatalysis and Biotransformation. 2008; 26(1–2):133–140.
27. Hemachandra LMP, et al. Mitochondrial Superoxide Dismutase Has a Protumorigenic Role in Ovarian Clear Cell Carcinoma. Cancer Research. 2015; 75(22):4973–4984. [PubMed: 26359457]
28. Chauvin B, et al. Plasma distribution of tetraphenylporphyrin derivatives relevant for Photodynamic Therapy: importance and limits of hydrophobicity. Eur J Pharm Biopharm. 2013; 83(2):244–52. [PubMed: 23089311]
29. Kessel D, et al. Tumor Localization and Photosensitization by Sulfonated Derivatives of Tetraphenylporphine. Photochemistry and Photobiology. 1987; 45(6):787–790. [PubMed: 3628502]
30. Winkelman J, Collins G. Neurotoxicity of tetraphenylporphinesulfonate TPPS4 and its relation to photodynamic therapy. Photochemistry and Photobiology. 1987; 46(5):801–807. [PubMed: 3441503]
31. Sema A. Experimental porphyric neuropathy: a preliminary report. Canadian Journal of Neurological Sciences. 1981; 8:105–114. [PubMed: 6271380]
32. Sortino S, et al. Nanoparticles of cationic amphiphilic cyclodextrins entangling anionic porphyrins as carrier-sensitizer system in photodynamic cancer therapy. Biomaterials. 2006; 27(23):4256–65. [PubMed: 16620960]
33. Kovaric B, et al. Self-Assembly of Peptide Porphyrin Complexes: Toward the Development of Smart Biomaterials. Journal of the American Chemical Society. 2006; 128(13):4166–4167. [PubMed: 16568957]
34. Hirohara S, et al. Synthesis, photophysical properties and sugar-dependent in vitro photocytotoxicity of pyrrolidine-fused chlorins bearing S-glycosides. J Photochem Photobiol B. 2009; 97(1):22–33. [PubMed: 19679489]
35. Ribó JM, et al. Aggregation in water solutions of tetrasodium diprotonated meso-tetrakis (4-sulfonatophenyl) porphyrin. Journal of the Chemical Society, Chemical Communications. 1994; (6):681–682.
36. Hollingsworth JV, et al. Characterization of the self-assembly of meso-tetra(4-sulfonatophenyl)porphyrin (H(2)TPPS(4-)) in aqueous solutions. Biomacromolecules. 2012; 13(1):60–72. [PubMed: 21995760]
37. Rice Z, Bergkvist M. Adsorption characteristics of a cationic porphyrin on nanoclay at various pH. Journal of colloid and interface science. 2009; 335(2):189–195. [PubMed: 19427642]
38. Xiang S, et al. Uptake mechanisms of non-viral gene delivery. Journal of Controlled Release. 2012; 158(3):371–378. [PubMed: 21982904]
39. Aggarwal LPF, Baptista MS, Borissevitch IE. Effects of NaCl upon TPPS4 triplet state characteristics and singlet oxygen formation. Journal of Photochemistry and Photobiology A: Chemistry. 2007; 186(2–3):187–193.

Highlights

- Cationic enzymatically synthesized glycogen (cESG) charge condensed TPPS for PDT
- cESG-TPPS improved light-induced cell death response, compared to unconjugated TPPS
- cESG-TPPS mediates PDT at dosages as low as 0.16 μM TPPS *in vitro*
- siRNA co-delivered with cESG-TPPS resulted in protein knockdown and efficient PDT

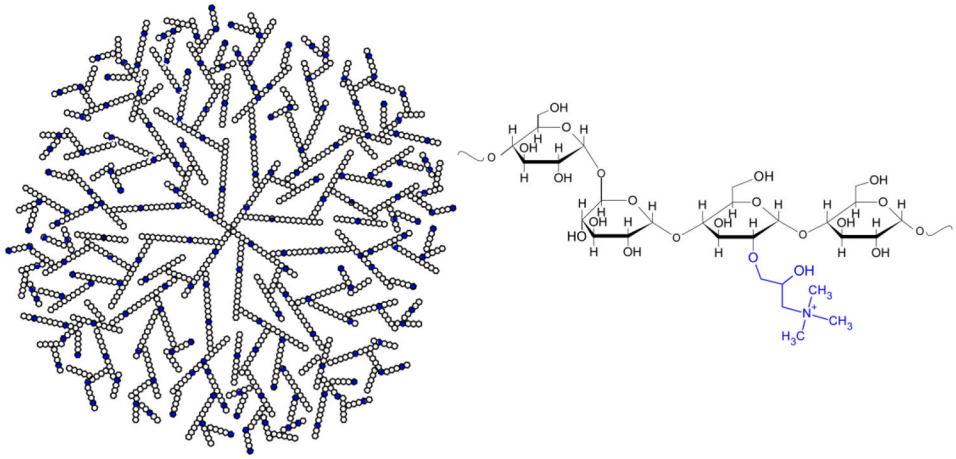

Figure 1.
Schematic of cESG dendrimeric structure. Blue indicates modification of residue with a quaternary ammonium group.

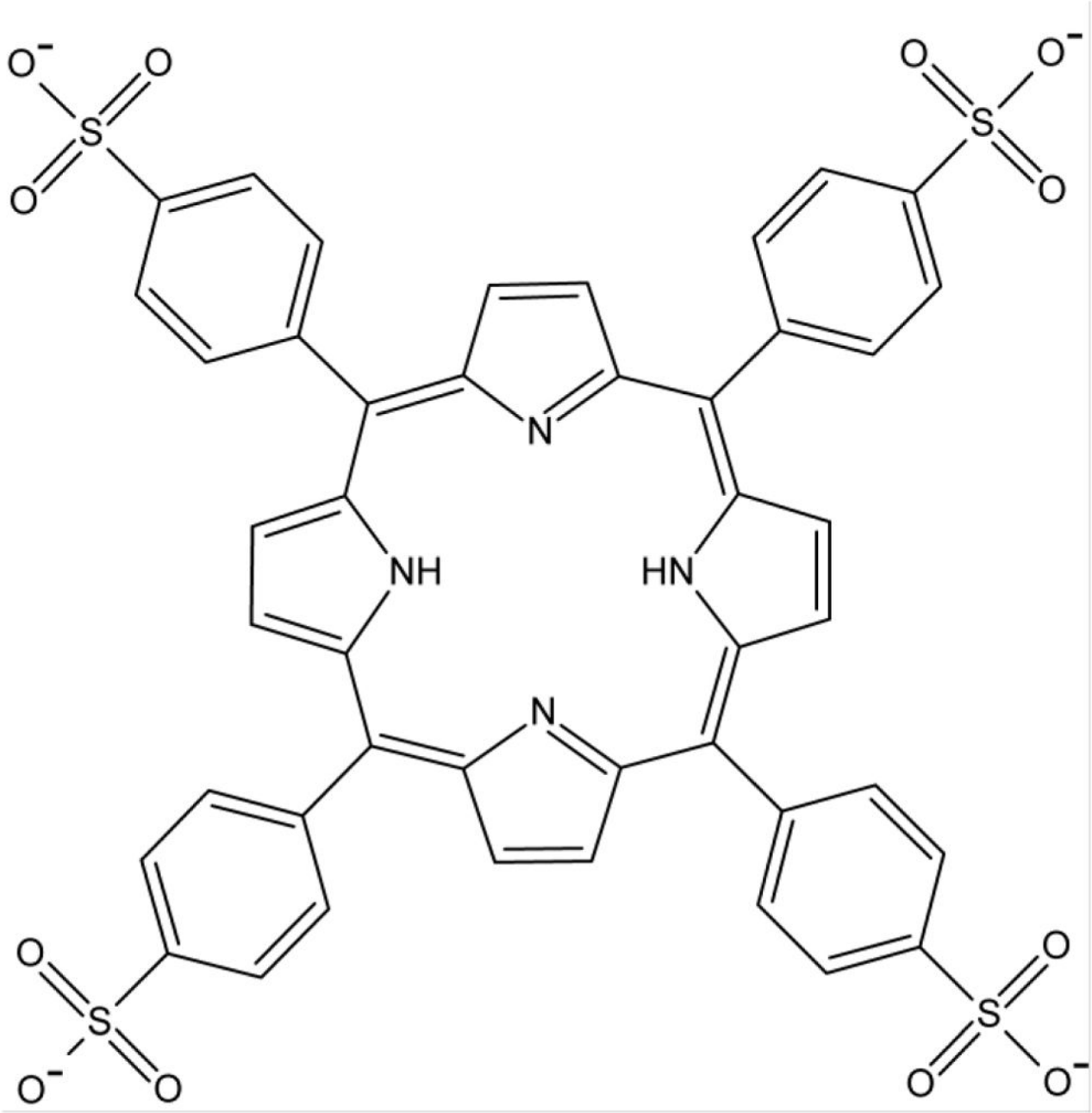

Figure 2.
Structure of TPPS (meso-tetra(4-sulfonatophenyl)porphyrin)

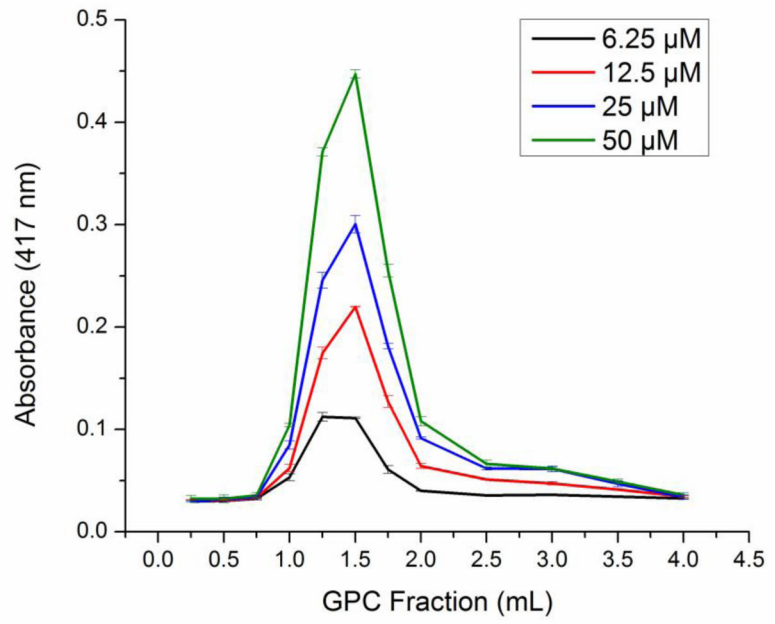

Figure 3.

GPC elution profile of cESG-TPPS detected by absorbance (417 nm) indicates that the amount of TPPS bound increased with higher concentrations of TPPS added (legend to the right). Mean ± standard deviation, n=3 absorbance measurements of representative replicate experiment.

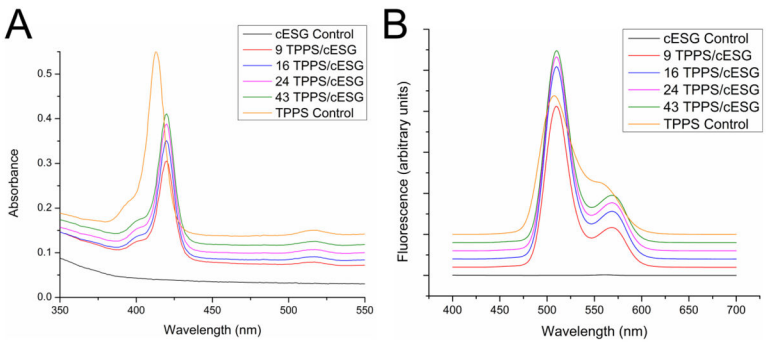

Figure 4.

Absorbance (A) and fluorescence emission spectra at 420 nm excitation (B) of TPPS and cESG-TPPS formulations (3 μM TPPS). Spectra are stacked for visualization. cESG encapsulated TPPS exhibits a red shift in maximum absorbance of the Soret band. n=3 independent syntheses measured in triplicate.

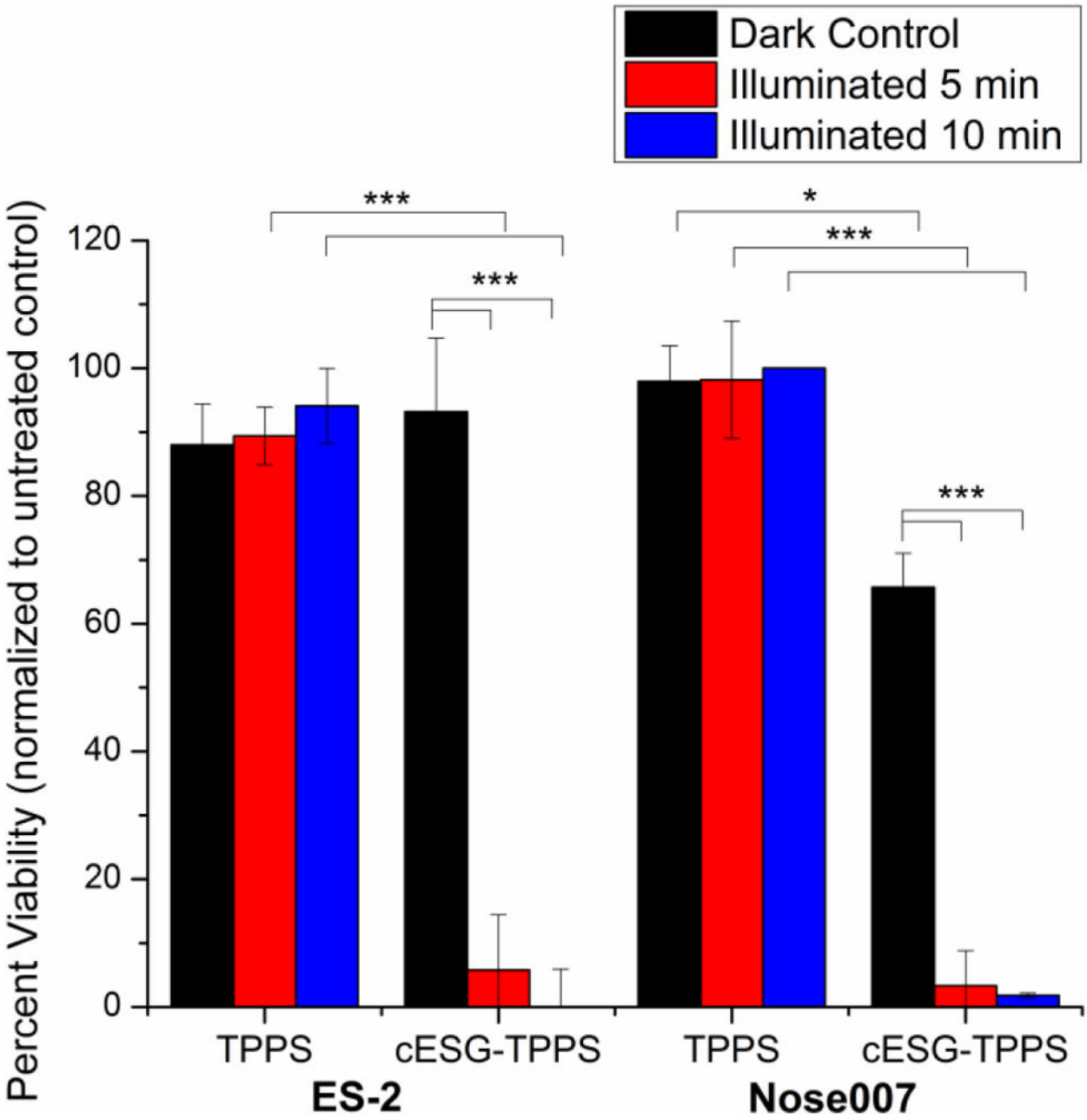

Figure 5.

TPPS conjugation to cESG improved PDT response in mammalian cell lines at different illumination times. MTT viability of cESG-TPPS or TPPS control treated ES-2 (left) and Nose007 cells (right) at 0.72 μM TPPS (2.7 nM cESG). Cells were treated overnight in growth media, followed by light treatment in fresh growth media. Viability was assessed 48 h after initiating treatment. n=3 independent experiments *p<0.05 **p<0.01 ***p<0.001 determined by one-way ANOVA with Tukey's post-hoc test.

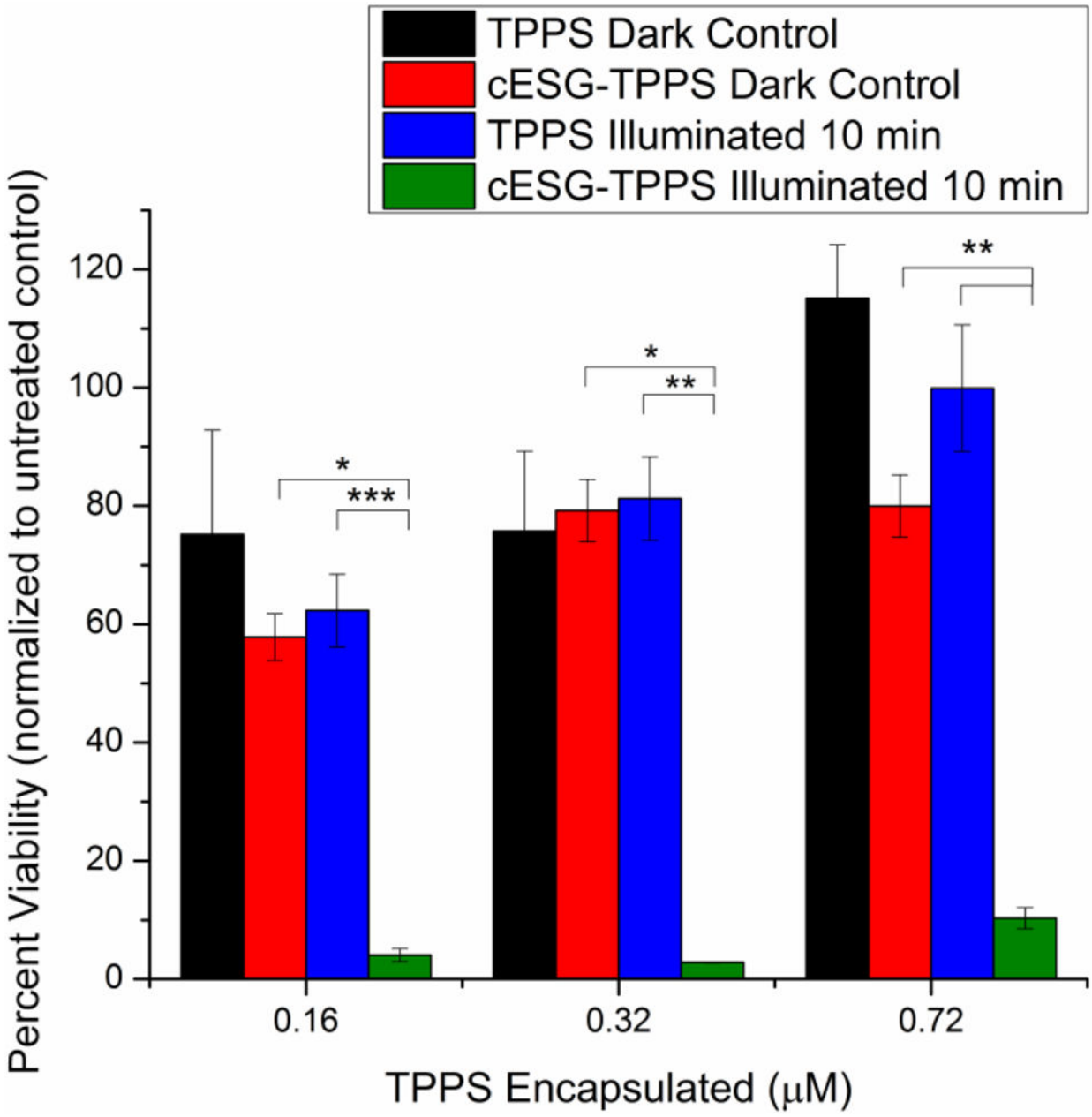

Figure 6.

cESG-TPPS improved PDT response over free TPPS at varying concentrations. MTT viability of cESG-TPPS and TPPS control treated ES-2 cells at constant concentration cESG (3.2 nM). Cells were treated overnight in growth media, followed by light treatment for 10 minutes in fresh growth media. Viability was assessed 48 h after initiating treatment. n=3 independent experiments *p<0.05 **p<0.01 ***p<0.001 determined by one-way ANOVA with Tukey's post-hoc test

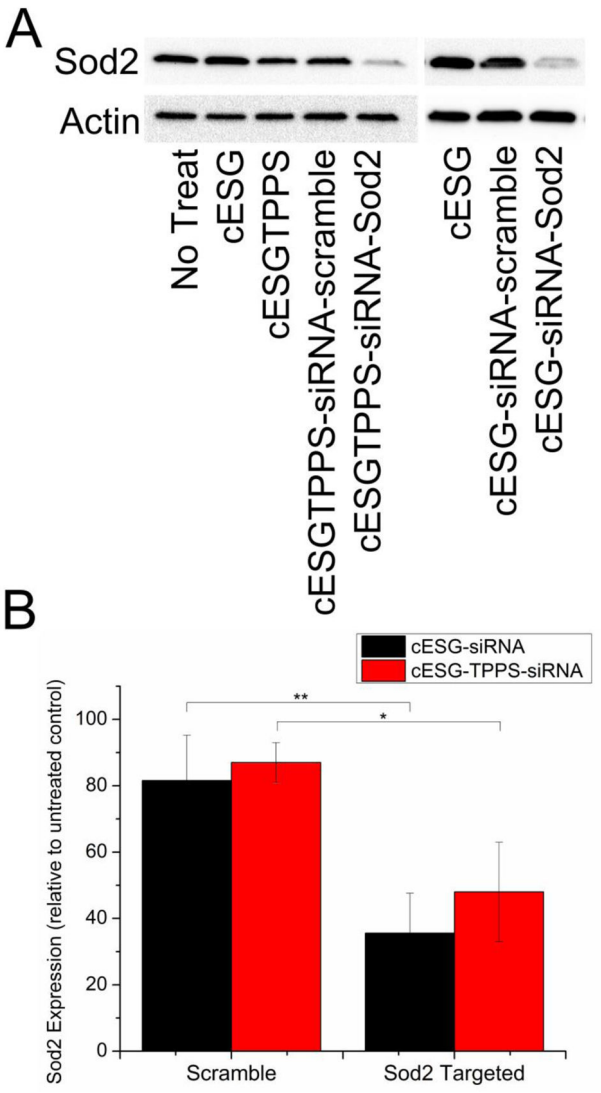

Figure 7.

TPPS conjugation did not interfere with siRNA delivery of cESG-TPPS-siRNA A) cESG-TPPS-siRNA facilitated knockdown of Sod2 protein expression similarly to cESG-siRNA in ES-2. Cells were treated for 72 hrs prior to assessment of Sod2 protein expression by western blotting. B) Western blot data was quantified by densitometric analysis and normalized to expression of the loading control β-Actin. Values were expressed relative to Sod2 expression in untreated control. (Mean ± standard deviation. n=3 experiments. *$p<0.1$ **$p<0.05$ determined by one-way ANOVA with Tukey's post-hoc test.) cESG-siRNA data previously reported [25]

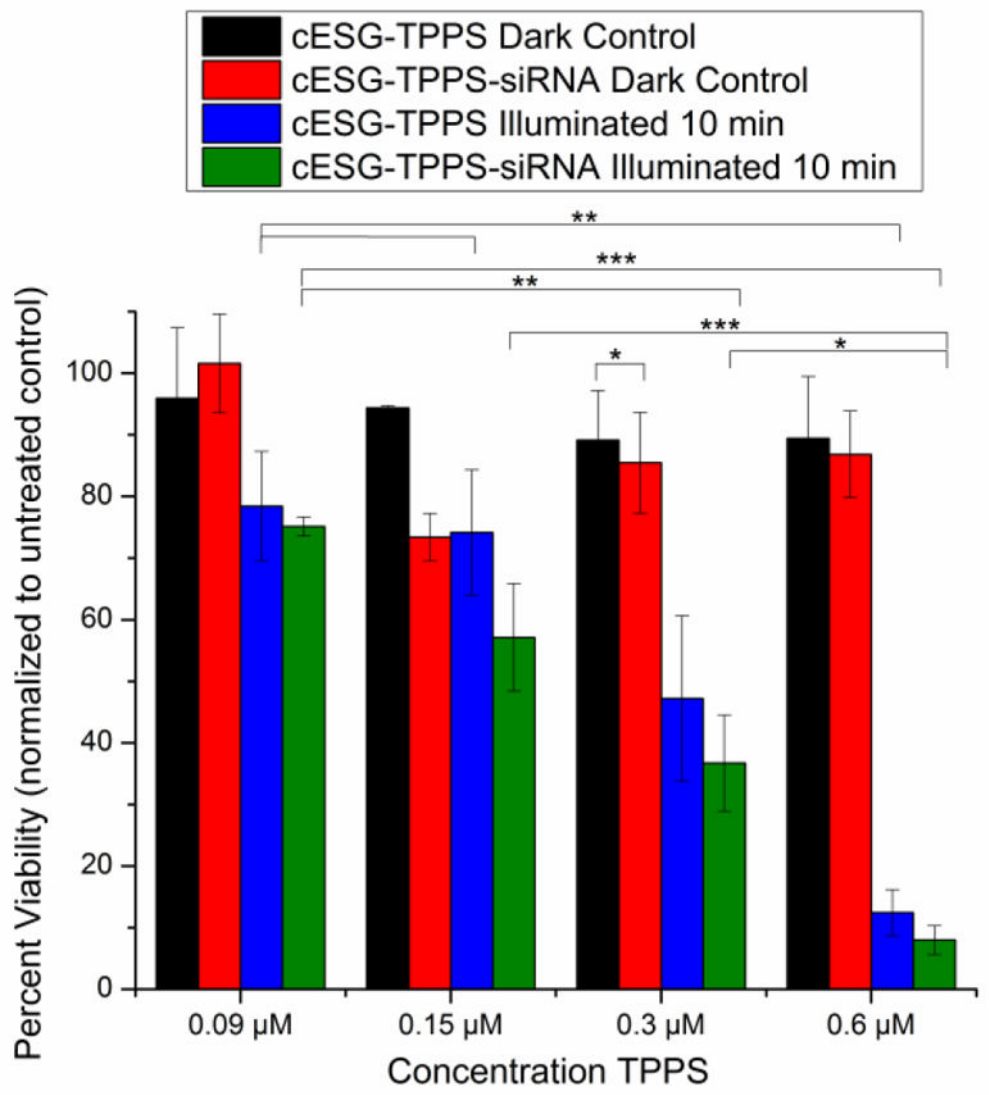

Figure 8.

Incorporation of siRNA did not interfere with TPPS PDT activity. ES-2 ovarian carcinoma cells treated for 72 hours with cESG-TPPS or cESG-TPPS-siRNA (siRNA targeted at Sod2) prior to 10 minute illumination with light. MTT viability was assessed 24 h after light treatment (Mean ± SEM, n=4 independent experiments. *p<0.05 **p<0.01 ***p<0.001 determined by one-way ANOVA with Tukey's post-hoc test).

Table 1

Size and Zeta Potential of cESG-TPPS[a]

TPPS (μM) Reacted with 0.78 μM cESG	Average TPPS Encapsulated (μM) ± Standard Deviation	Encapsulation Efficiency (%)	Size ± Standard Deviation	Zeta Potential ± Standard Deviation
0	0	n/a	37.0 ± 11.8	20.2 ± 2.9
6.25	7.0 ± 2.7	112	41.4 ± 8.5	4.4 ± 4.2
12.5	12.2 ± 5.1	98	44.5 ± 10.8	5.2 ± 1.5
25	19.0 ± 5.5	76	35.7 ± 0.4	4.6 ± 3.8
50	33.4 ± 6.0	67	45.6 ± 10.9	4.4 ± 4.0

[a] n=3 independent syntheses measured in triplicate in 1 mM sodium phosphate buffer

Table 2

Size and Zeta Potential of cESG-TPPS-siRNA Complexes with Varying TPPS Concentration.[a]

cESG-TPPS-siRNA TPPS per particle	Size ± Standard Deviation (nm)	Zeta Potential ± Standard Deviation (mV)
9	51.2 ± 5.5	0.03 ± 15.1
16	56.4 ± 3.3	3.6 ± 32.1
24	36.1 ± 4.1	0.2 ± 14.3
43	37.7 ± 3.0	2.0 ± 22.3

[a] cESG and siRNA concentration held constant, 4 siRNA per particle. Results were averaged over three measurements.